

## MODELING OF A HIGH SPEED TROLLEY, REMOTE-HEAD AND CAMERA SYSTEM

**Vitor Ferreira Romano, romano@mecanica.ufrj.br**

Federal University of Rio de Janeiro – Poli/UFRJ  
Mechanical Engineering Department, Robotics Laboratory  
Cidade Universitária – CT, Bloco G-204 - 21945-970 Rio de Janeiro - RJ – Brazil

**Eugênia Cruz da Trindade, eugenia.trindade@fmcti.com**

FMC Technologies do Brasil  
Rod. Presidente Dutra 2660  
21538-900 - RJ - Brazil

**Abstract.** This paper presents some results of the kinematics and dynamic modeling of a high speed broadcast equipment to be used for TV transmission of 100 meters athletics race. This equipment is formed by a digital camera, a pan-tilt remote-head and a high speed wheeled trolley moving along a binary linear track fixed on the floor. A complete kinematics model of the system described in homogeneous transformation matrices was used in the analysis. The 2D mathematical dynamic modeling of complete system is calculated in the runner reference frame and includes the trolley dynamics and its state-space modeling. Elastic deformations due to binary track bending and track surface irregularities were also studied. The parameters used in the model are based on a real project of a low speed telerobotic camera trolley system. Some results of the simulations are also presented.

**Keywords:** camera trolley, cine-video equipment, dynamic modeling, mechatronics, teleoperation.

### 1. INTRODUCTION

Athletism represents the millenary tradition of Olympic Games and undoubtedly is one of the most watched sport competitions on TV. Official athletics competitions are performed in standard fields certified by the IAAF – International Association of Athletics Federation -. In general they are ovals of 400 meters in circumference, made with a rubberized surface and normally consist of 8 to 10 lanes with 9.78 meters large (Fig. 1).



Figure 1. Athletic field and equipment location.

The television networks demand for sophisticated equipments to generate and transmit high quality images with different and exclusive view angles. Regarding 100 meters split athletics race, low height images of the runners feature special scenes of the competition, as presented in Fig. 2a.

Equipments consisting on a high speed wheeled trolley moving along a binary linear track with a camera installed on a pan-tilt remote-head located onboard the trolley, have been frequently used to generate these images (Fig.2b). Camera-trolley systems are usually installed near the field, fixed on the floor and occupy the region signed in Fig.1, corresponding to nearly 210 meters length, with an operational travel distance of approximately 120 meters.



Figure 2. (a) Camera image at low height. (b) Camera-trolley system.

## 2. GENERAL ASPECTS

A camera trolley system is here considered as equipment comprised of a high definition camera, a two axis (pan-tilt) remote-head and a trolley (vehicle) with wheels and counter-wheels, moving along track modules formed by binary tracks (tubes) and structural elements (Fig. 3). Motion can be provided by a cable and pulley mechanism actuated by electrical motor. The trolley position and velocity control is classified as teleoperated mode (open-loop control). The cameraperson sends command signals from a control panel to the trolley onboard microcontroller able to operate different acceleration ramps (Romano et al, 2004).

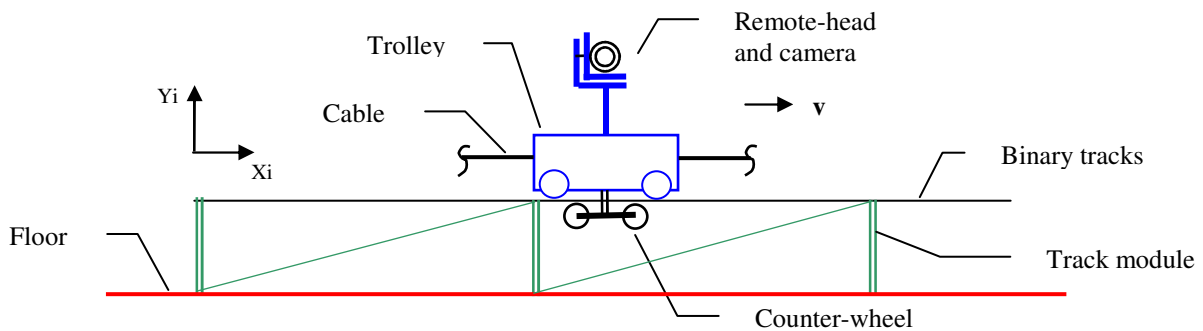


Figure 3. Concept of the camera-trolley system.

The conceptual design of a camera-trolley system must consider the existence of external perturbations, such as linear and angular mechanical vibrations due to binary track geometrical discontinuities. Other important aspects are related to uncertainties due to the installation of the track mounting parts and structural stiffness of the whole system (Fig. 4).

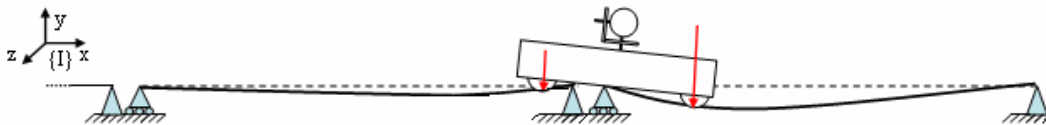


Figure 4. Binary track structural deformation (bending).

The biggest challenge for the development of this project is to provide acceptable range values of external perturbations when the system is operated, in order not to create undesired fluctuations of the runner image. High precision mechanical components and vibration absorbers are often the key solutions to minimize the problems.

The quality of the runner image also depends on cameraperson skills to deal with three optical parameters (focus, zoom and iris) of the camera-lens unit and the position and velocity control of the three degrees-of-freedom mechanical parameters (trolley translation, pan and tilt remote-head angles) of the equipment.

Focus and zoom are the most important operational parameters regarding image quality. The focal length of a lens determines its angle of view, and thus also how much an image detail will be magnified for a given scene position. Wide-angle lenses are more indicated to this application, since they have small focal lengths, while telephoto lenses

have larger corresponding focal lengths and then are more susceptible to camera shake since small amplitudes become magnified within the image.

### 3. KINEMATICS MODEL

#### 3.1. Trolley

The position and orientation of the trolley body in absolute coordinates, reference  $\{I\}$ , can be modeled as a two degrees-of-freedom (d.o.f.) system, consisting in a vertical translation of the system center of mass (cm) and a rotation around this point, given by  $y_{cm}$  and  $\theta_{cm}$  respectively (Fig. 5). The linear position (X direction) of the trolley system is given by the parameter  $x_{cm} = s(t)$ .

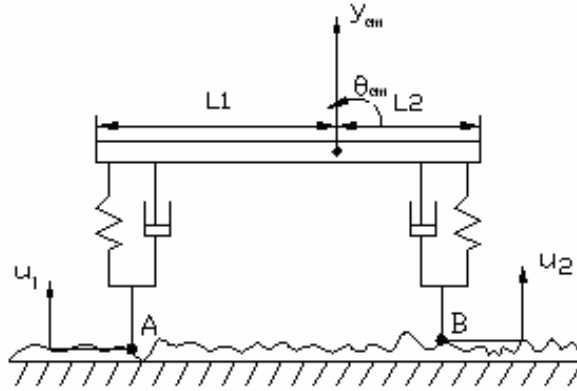


Figure 5. 2D model of the trolley.

Homogeneous transformation matrices (Sciavicco and Siciliano, 2001) can describe the kinematical relations of the parts. The trolley parameters are represented by:

- matrix  ${}^I T_0$ : relating the position  $x_{cm}$  of the center mass reference frame  $\{0\}$  to the global inertial reference frame  $\{I\}$ .
- matrix  ${}^0 T_1$ : frame  $\{1\}$  related to frame  $\{0\}$  (translation  $y_{cm}$ ).
- matrix  ${}^1 T_2$ : frame  $\{2\}$  related to frame  $\{1\}$  (rotation  $\theta_{cm}$ ).

The final expression in global inertial reference frame  $\{I\}$ , is given by:

$${}^I T_2 = {}^I T_0 \cdot {}^0 T_1 \cdot {}^1 T_2 \quad (1)$$

#### 3.2. Pan-tilt remote-head

The pan-tilt remote-head is a 2 d.o.f. mechanism used to move a camera in two orthogonal planes. The remote-head column (link 2) is rigidly fixed to the trolley and an actuator (electrical motor) connected to a rotational joint provides the link 3 motion, associated to pan ( $\theta_p$ ) angular displacement. The camera is fixed to tilt platform (link 4) and its motion is also made by a motor located at the rotational joint, given the tilt ( $\theta_t$ ) angular displacement. In the kinematics model the pan mechanism is described by frame  $\{3\}$  and the tilt mechanism by frame  $\{4\}$ , as presented in Fig. 6a. The frame  $\{4\}$  can be located in the camera view axis, for convenience. The remote head homogeneous transformation matrix is represented by:

- matrix  ${}^2 T_3$ : frame  $\{3\}$  related to frame  $\{2\}$  (rotation  $\theta_p$ ).
- matrix  ${}^3 T_4$ : frame  $\{4\}$  related to frame  $\{3\}$  (rotation  $\theta_t$ ).

Then,

$${}^2 T_4 = {}^2 T_3 \cdot {}^3 T_4 \quad (2)$$

#### 3.3. Ideal kinematics model

In Fig. 6 are defined the position and orientation of the local reference frames for the trolley and pan-tilt remote head. The global homogeneous transformation matrix  ${}^I T_4$ , which describes the camera view axis position and orientation in the global inertial reference frame  $\{I\}$  is given by:

$${}^I T_4 = {}^I T_0 \cdot {}^0 T_1 \cdot {}^1 T_2 \cdot {}^2 T_3 \cdot {}^3 T_4 \quad (3)$$

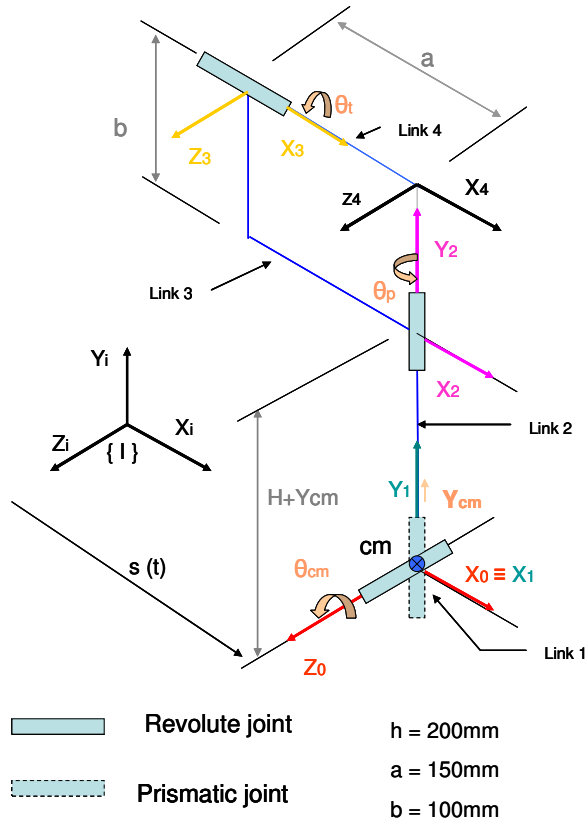


Figure 6. Local and inertial reference frames (ideal model).

### 3.4. Track bending effect

Bending occurs whenever the trolley system passes over the binary track, causing a structural deformation that disturbs the position (translation  $Y_{tr}$ ) and orientation (rotation  $\theta_{tr}$ ) of the trolley center mass reference frame  $\{0\}$  related to the global inertial reference frame  $\{I\}$ , as mentioned in equation (1).

The homogeneous transformation matrices associated to the bending effect, in the global inertial reference frame  $\{I\}$ , can be defined as:

- matrix  ${}^1T_0$ : relating the position  $x_c$  of the center mass reference frame  $\{0\}$  to the global inertial reference frame  $\{I\}$ .
- matrix  ${}^0T_{t1}$ : frame  $\{t1\}$  related to frame  $\{0\}$  (rotation  $\theta_{tr}$ ).
- matrix  ${}^{t1}T_{t2}$ : frame  $\{t2\}$  related to frame  $\{t1\}$  (translation  $Y_{tr}$ ).
- matrix  ${}^{t2}T_1$ : frame  $\{1\}$  related to frame  $\{t2\}$  (translation  $y_{cm}$ ).

Resulting in,

$${}^1T_1 = {}^1T_0 \cdot {}^0T_{t1} \cdot {}^{t1}T_{t2} \cdot {}^{t2}T_1 \quad (4)$$

The matrix  ${}^0T_1$  was redefined to include the structural deformations.

### 3.5. Complete kinematics model

The complete homogeneous transformation matrix with track bending effect, in the global inertial reference frame  $\{I\}$ , is given by:

$${}^1T_4 = {}^1T_0 \cdot {}^0T_{t1} \cdot {}^{t1}T_{t2} \cdot {}^{t2}T_1 \cdot {}^1T_2 \cdot {}^2T_3 \cdot {}^3T_4 \quad (5)$$

or

$${}^1T_4 = \begin{pmatrix} \cos(\theta_{cm} + \theta_{tr}) \cos(\theta_p) & -\cos(\theta_t) \text{sen}(\theta_{cm} + \theta_{tr}) + \cos(\theta_{cm} + \theta_{fa}) \text{sen}(\theta_p) \text{sen}(\theta_t) & & & \\ \text{sen}(\theta_{cm} + \theta_{tr}) \cos(\theta_p) & \cos(\theta_t) \cos(\theta_{cm} + \theta_{tr}) + \sin(\theta_{cm} + \theta_{tr}) \text{sen}(\theta_p) \text{sen}(\theta_t) & & & \\ -\text{sen}(\theta_p) & & \text{sen}(\theta_t) \cos(\theta_p) & & \\ 0 & & 0 & & \\ \cos(\theta_t) \cos(\theta_{cm} + \theta_{tr}) \text{sen}(\theta_p) + \text{sen}(\theta_{cm} + \theta_{tr}) \text{sen}(\theta_t) & s(t) - (b + H + y_{tr} + y_{cm}) \text{sen}(\theta_{cm} + \theta_{tr}) & & & \\ \cos(\theta_t) \text{sen}(\theta_{cm} + \theta_{tr}) \text{sen}(\theta_p) - \cos(\theta_{cm} + \theta_{tr}) \text{sen}(\theta_t) & (b + H + y_{tr} + y_{cm}) \cos(\theta_{cm} + \theta_{tr}) & & & \\ \cos(\theta_t) \cos(\theta_p) & & 0 & & \\ 0 & & 1 & & \end{pmatrix} \quad (6)$$

### 3.6. Runner reference

In Fig. 7 and Fig. 8 are illustrated the pan and tilt angular motions of the camera and remote-head unit needed to observe the desired target, a runner located in the first lane (reference {5}), in terms of vector position  ${}^4P_5$  ( $\mathbf{r}$  vector) or focal distance relative to the camera reference frame {4}. This position vector describes the runner position in the inertial reference frame {0}, with the use of homogeneous transformation matrix  ${}^1T_4$ , as follows:

$${}^1P_5 = {}^1T_4 \cdot {}^4P_5 \quad (7)$$

with

$${}^4P_5 = [0 \ 0 \ r \ 1]^T$$

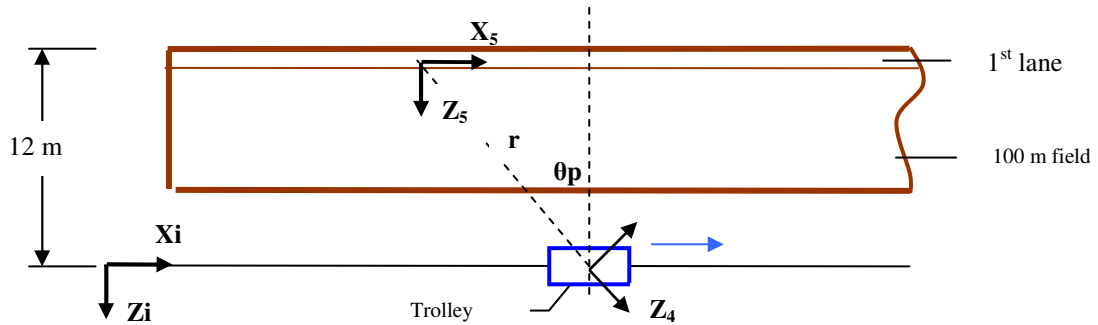


Figure 7. Pan angle  $\theta_p$  and focal distance  $r$  from runner to camera.

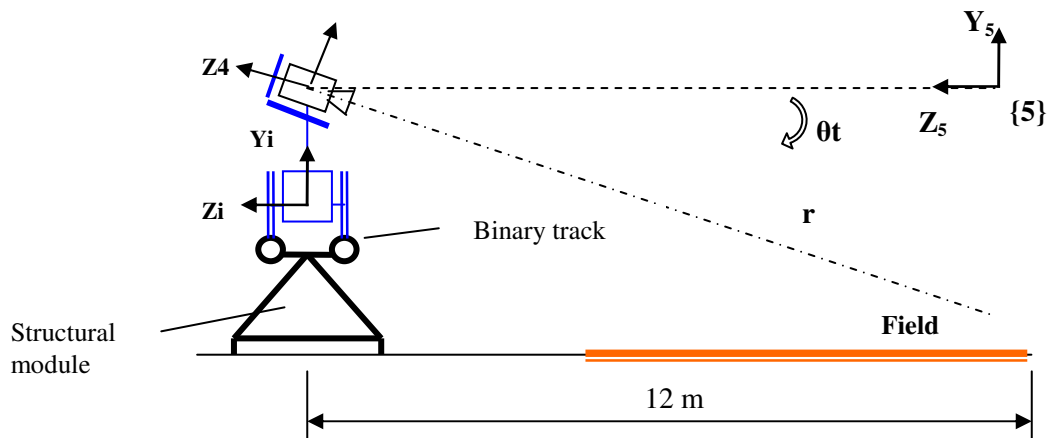


Figure 8. Tilt angle  $\theta_t$  and focal distance  $r$  from runner to camera.

The global homogeneous transformation matrix  ${}^1T_4$  and the position vector describing the runner position in the inertial reference frame {0} (Eq.6) were calculated with Mathematica® program for the following configurations:

- configuration 1:  $\theta_p = \theta_t = 0$ .

- configuration 2:  $\theta_p = \pi/6$  and  $\theta_t = 0$ .
- configuration 3:  $\theta_p = \pi/3$  and  $\theta_t = 0$ .
- configuration 4:  $\theta_p = \pi/3$  and  $\theta_t = 0.04$  rad. (focus point at the runner feet).

### 3. DYNAMIC MODEL

#### 3.1. Dynamic equations

A 2D dynamic model of a wheeled trolley moving along a binary linear track fixed on the floor (Romano, Trindade, 2006) is presented in Fig. 5. The same model can be used in the complete system, since the remote-head and camera are considered as rigid bodies connected to the trolley. The system force diagram is described in Fig. 9.

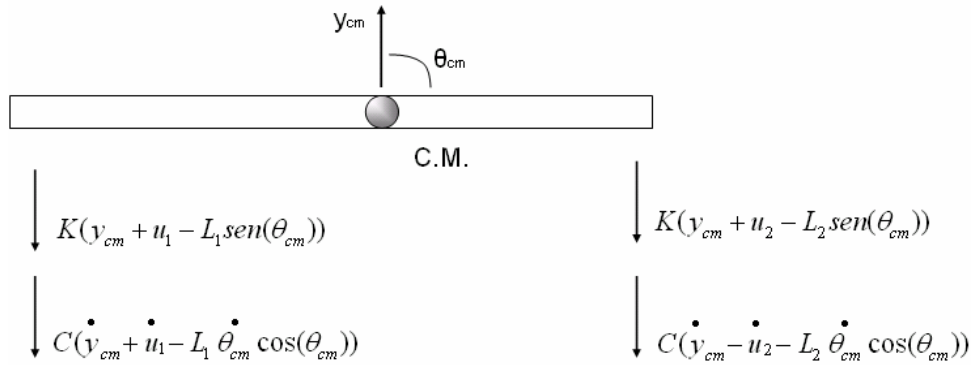


Figure 9. Force diagram.

The force and momentum equilibrium conditions in Fig. 9 - equations (8) and (9) respectively - are:

$$\sum F = m \ddot{y}_{cm}$$

$$m \ddot{y}_{cm} = -K(2y_{cm} + u_1 - L_1 \theta_{cm} - u_2 - L_2 \theta_{cm}) - C(2\dot{y}_{cm} + \dot{u}_1 - \dot{u}_2 - L_1 \dot{\theta}_{cm} + L_2 \dot{\theta}_{cm}) \quad (8)$$

$$\sum M_F^{cm} = J \ddot{\theta}_{cm}$$

$$J \ddot{\theta}_{cm} = K[L_1(y_{cm} + u_1 - L_1 \theta_{cm}) - L_2(y_{cm} - u_2 - L_2 \theta_{cm})] + C[L_1(\dot{y}_{cm} + \dot{u}_1 - L_1 \dot{\theta}_{cm}) - L_2(\dot{y}_{cm} - \dot{u}_2 - L_2 \dot{\theta}_{cm})] \quad (9)$$

where

C: damping coefficient

J: moment inertia

K: rigidity coefficient

M: mass

F: resultant forces at trolley

$M_F^{cm}$ : resultant torques at trolley center mass

#### 3.2. State space equations

The trolley dynamic model is a multivariable system, so that state space equations can be used to describe its behavior. The state differential and output equations are described in Eq. (10) and Eq. (11) (Dorf, and Bishop, 2001).

$$\dot{x}(t) = Ax(t) + Bu(t) \quad (10)$$

$$y(t) = Cx(t) + Du(t) \quad (11)$$

Then, the mathematical model for the trolley in matrix form is:

$$\dot{x}(t) = \begin{bmatrix} 0 & 1 & 0 & 0 \\ -\frac{2K}{M} & -\frac{2C}{M} & \frac{K(L_1-L_2)}{M} & -\frac{C(L_1-L_2)}{M} \\ 0 & 0 & 0 & 1 \\ \frac{K(L_1-L_2)}{I} & \frac{C(L_1-L_2)}{I} & -\frac{K(L_1^2-L_2^2)}{I} & -\frac{C(L_1^2-L_2^2)}{I} \end{bmatrix} x(t) + \begin{bmatrix} -\frac{C}{M} & \frac{C}{M} \\ \left(\frac{2C^2}{M^2} + \frac{C^2L_1(L_1-L_2)}{M} + \frac{K}{M}\right) & \left(-\frac{2C^2}{M^2} + \frac{C^2L_2(L_1-L_2)}{M} + \frac{K}{M}\right) \\ \frac{CL_1}{I} & \frac{CL_2}{I} \\ \left(\frac{-C^2(L_1-L_2)}{M} - \frac{C^2L_1(L_1^2-L_2^2)}{I^2} + \frac{KL_1}{I}\right) & \left(\frac{C^2(L_1-L_2)}{M} - \frac{C^2L_2(L_1^2-L_2^2)}{I^2} + \frac{KL_2}{I}\right) \end{bmatrix} u(t) \quad (12)$$

and

$$\begin{bmatrix} y(t) \\ \theta(t) \end{bmatrix} = \begin{bmatrix} 1 & 0 & 0 & 0 \\ 0 & 0 & 1 & 0 \end{bmatrix} x(t) + \begin{bmatrix} 0 & 0 \\ 0 & 0 \end{bmatrix} u(t) \quad (13)$$

## 4. STRUCTURAL ANALYSIS

### 4.1. Vibration model

The vertical displacements of the wheels (points A and B) are the system excitation input parameters. To obtain the vibration model equations, the expressions (8) and (9) are calculated for the condition  $u_1 = u_2 = 0$ , resulting:

$$m\ddot{y}_{cm} + 2C\dot{y}_{cm} - C(L_1 - L_2)\dot{\theta}_{cm} + 2Ky_{cm} - K(L_1 - L_2)\theta_{cm} = 0 \quad (14)$$

$$J\ddot{\theta}_{cm} - C(L_1 - L_2)\dot{y}_{cm} + C(L_1^2 + L_2^2)\dot{\theta}_{cm} - K(L_1 - L_2)y_{cm} + K(L_1^2 - L_2^2)\theta_{cm} = 0 \quad (15)$$

or in matrix form:

$$\begin{bmatrix} M & 0 \\ 0 & J \end{bmatrix} \begin{bmatrix} \ddot{y}_c \\ \ddot{\theta}_c \end{bmatrix} + \begin{bmatrix} 2C & -C(L_1-L_2) \\ -C(L_1-L_2) & C(L_1^2-L_2^2) \end{bmatrix} \begin{bmatrix} \dot{y}_c \\ \dot{\theta}_c \end{bmatrix} + \begin{bmatrix} 2K & -K(L_1-L_2) \\ -K(L_1-L_2) & K(L_1^2-L_2^2) \end{bmatrix} \begin{bmatrix} y_c \\ \theta_c \end{bmatrix} = \begin{bmatrix} 0 \\ 0 \end{bmatrix} \quad (16)$$

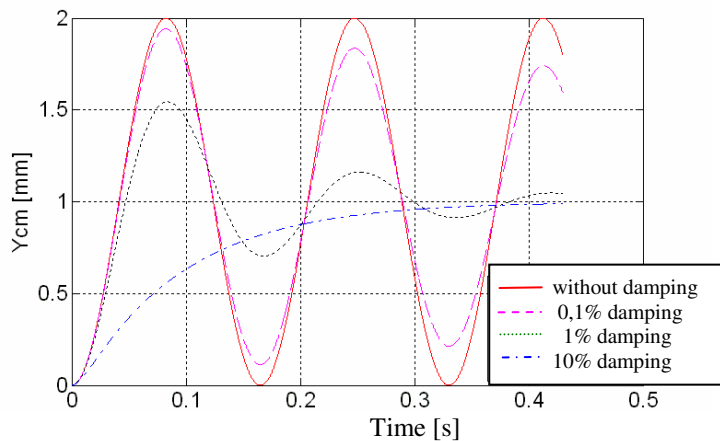


Figure 10. Time domain simulation. Natural frequency of 38,04 rad/s.

## 4.2. Track bending

Track elastic deformations (bending) are included in the model, but only the static formulations were considered in the analysis.

The external loads at the track are caused by the trolley weight applied at the contact points originated at wheels and track interface. Tracks are assumed to be weightless.

The loads exerted by the trolley wheels vary according their positions along the track, as presented in Fig. 11.

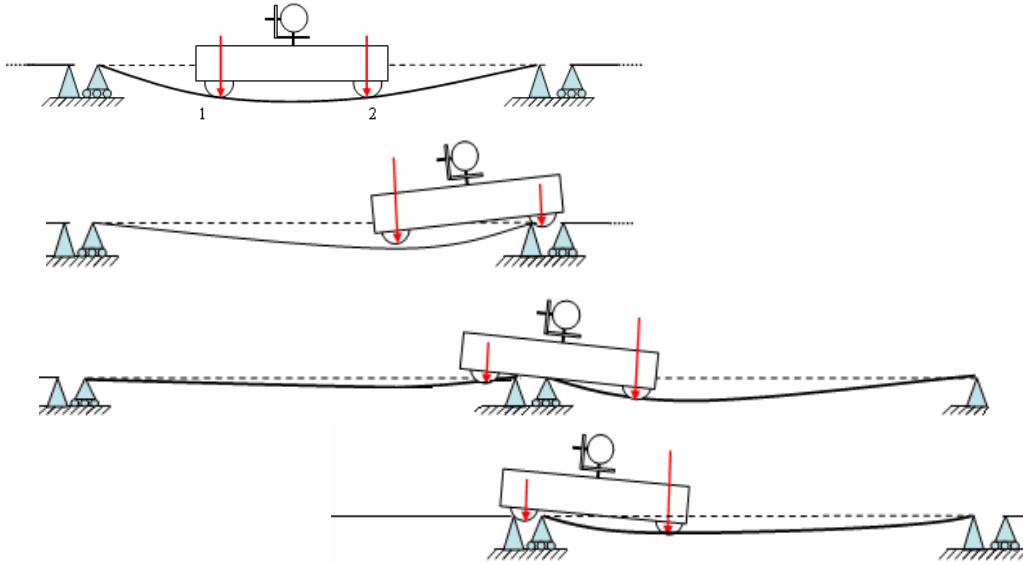


Figure 11. Load distribution along the track.

Center mass deviation  $y_{tr}$  due to bending can be calculated by equation 17, where  $y_1$  and  $y_2$  [mm] are the structural deformation due to wheels contact points (Fig. 12a).  $Y_{tr}$  values are plotted in Figure 12b. Similar procedure is used to calculate the angular deformation  $\theta_{tr}$ .

$$y_{tr}(t) = \frac{y_1(t) + y_2(t)}{2} \quad (17)$$

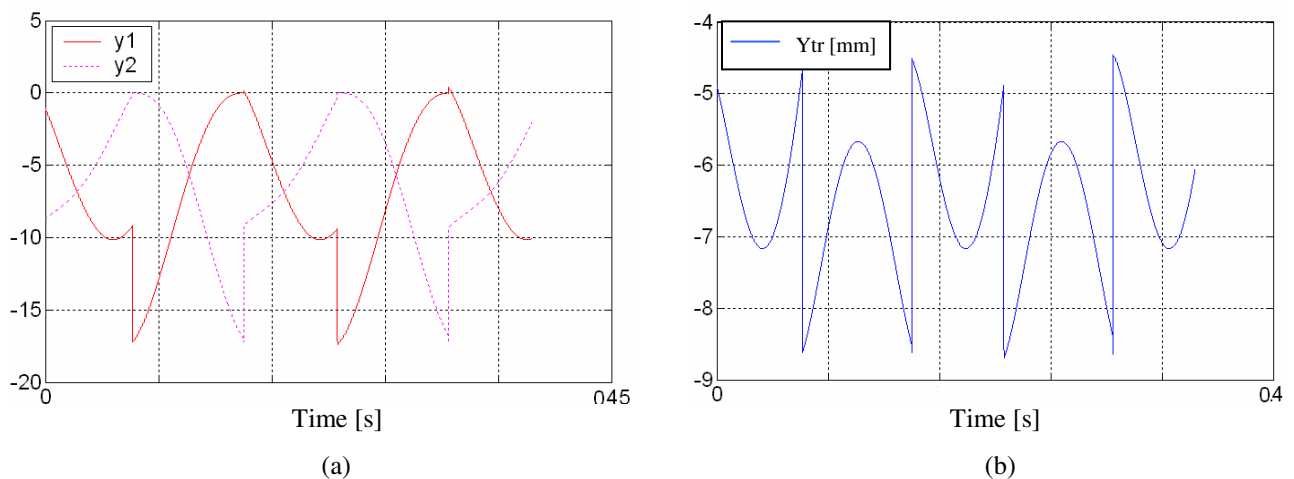


Figure 12. Structural deformation. (a) Values for wheels 1 and 2. (b) Calculated value at mass center point.

## 5. MODEL SIMULATION

### 5.1. Input parameters

The system is influenced by two main excitation input functions: the fluctuation of displacements due to surface irregularities and the existing space at the tracks for thermal expansion.

Kinematics parameters are associated to the pan  $\theta_p$  and tilt  $\theta_t$  remote-head motion, the distance of the runner to be focused in relation to the camera view axis, and the controlled velocity of the trolley.

The system total mass (including onboard equipment) is estimated in 60 kg.

#### 5.1.1. Tube and track interface

The main components of the binary tracks are commercial tubes that are successively connected to the track modules. During summer the temperature of the tracks can change from 15°C to 60°C, therefore a special fixture device was conceived to separate appropriately the tube and track modules interfaces, so that the necessary thermal expansion could occur. A space of 2.0 mm was chosen to guarantee the necessary separation of the parts.

The amplitude of the vertical motion of the camera trolley system, due to the passage of the wheel in the 2.0 mm space (impact neglected) was calculated as 0.014 mm (Romano and Trindade, 2004).

#### 5.1.2. Non-linear displacements

The non-linear displacements  $u_1$  and  $u_2$  consists on elastic deformations of the whole system, track surface irregularities such as ovalization and roughness, and the space for thermal expansion at the tracks. Due to the unpredictable nature of these parameters, they were modeled as a trigonometric function with amplitude of 0.5 mm and a discontinuity related to the space for thermal expansion.

### 5.2. Simulation results

The main output data of the model consist on the position of the system center of mass  $x_{cm} = s(t)$ , the translation  $y_{cm}$  and the rotation  $\theta_{cm}$  around this point, the position and orientation of frame {4} relative to frame {I}, and the position  $[x_5, y_5, z_5]^T$  of the runner in absolute coordinates.

Simulation results are related to the dynamic model including the tube elastic deformation. An example is given in Fig. 13, where the  $y_{cm}$  translation of the trolley cm with 1% damping is correlated to different velocities.

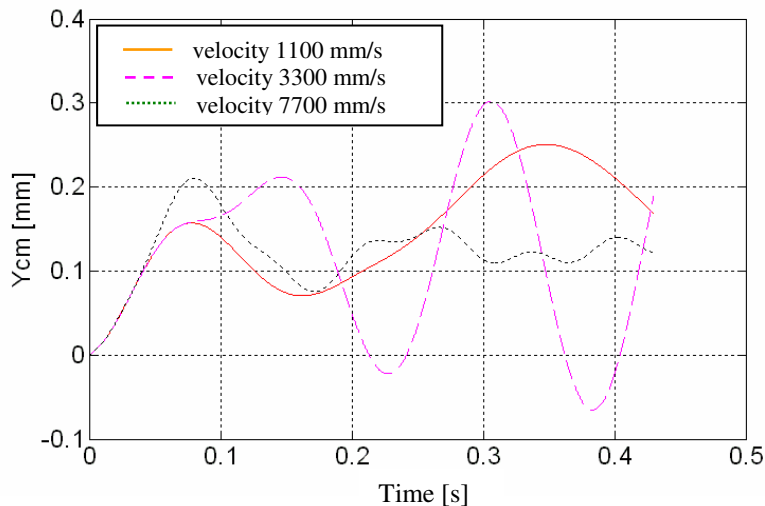


Figure 13. Translation  $y_{cm}$  with 1% damping for different trolley velocities.

In Figure 14 is presented the Y position of reference frame {4} in absolute coordinates for configuration 3 ( $\theta_p = \pi/3$  and  $\theta_t = 0$ ).

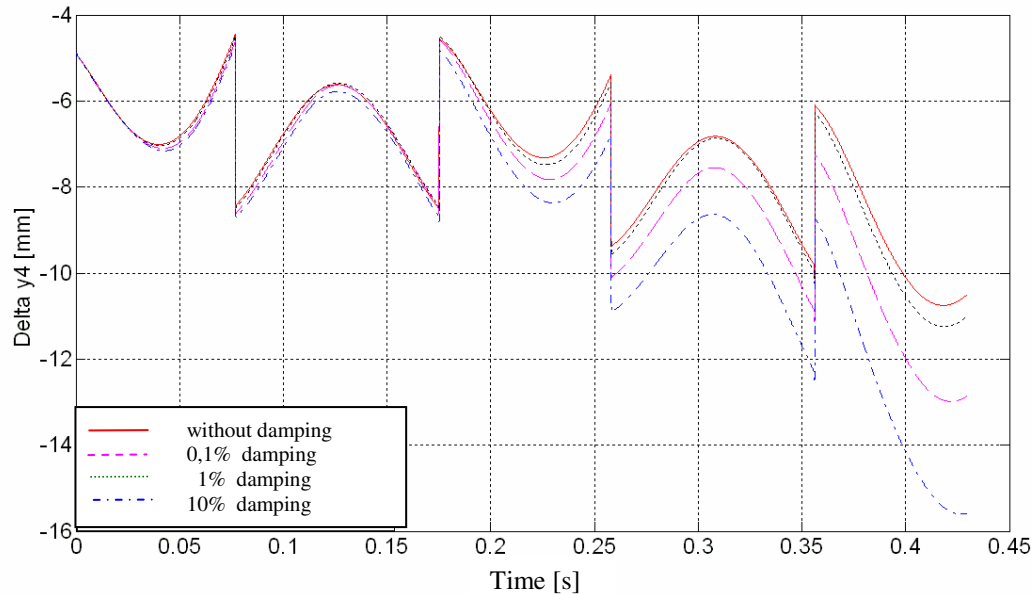


Figure 14. Position of reference frame {4} for  $\theta_p = \pi/3$  and  $\theta_t = 0$ .

## 6. CONCLUSIONS

Partial results of the simulations indicate the influence of the input parameters non-linearity (displacements  $u_1$  and  $u_2$ ), mainly related to track surface irregularities and the space for thermal expansion at the tracks, on the system dynamics. These input parameters will increase the amplitudes of the position coordinates of the observed image (output parameters  $x_5$  and  $y_5$ ) according to the different remote head pan and tilt angles and the focus distance associated to observed runner and camera center point. Also the non-linear influence of the elastic deformations on the track was included in the dynamic modeling. The position deviations can be drastically reduced with the appropriate use of counter-wheels, not considered in this paper. A complete simulation analysis is under development.

Since the high speed trolley system moves always forward in the same binary track during the image transmission, it is possible to design a low cost system, make a data acquisition procedure to record all the non-linear perturbations along the trajectory as many times as necessary to obtain a feasible database and establish an experimental model of the system behavior. Then, the next step can be the implementation of a control strategy based on active control devices located onboard to compensate for the pre-processed perturbations related to a specific position and velocity of the trolley in the track.

The results here presented would also be useful to determine the most appropriate way to reduce the mechanical vibration of the trolley-track system to acceptable frequency and amplitude ranges, in order to guarantee stable TV images generated during its motion.

## 7. REFERENCES

- Beitz, W. and Küttner K.-H., Editors, 1994, "Dubbel Handbook of Mechanical Engineering", Springer-Verlag, U.K..  
 Cradall, S. H., Dahl, N. C., Lardner, T. J., "An Introduction to the Mechanics of Solids", 2<sup>nd</sup> Edition, Singapore, 1978.  
 Dorf, R.C., Bishop. R. H., 2001, "Modern Control Systems" (in Portuguese), Ed. LTC, pp. 93-127.  
 Meirovitch, L., "Elements of Vibration Analysis", New York, McGraw-Hill, 1975.  
 Ogata, K., "Engenharia de Controle Moderno", 3<sup>a</sup> edição, Rio de Janeiro, Editora LTC, 2000.  
 Romano, V.F., Ferreira, C.V., Ferreira, C.G., 2003, "Mechatronic Design of a Telerobotic Trolley for the TV Transmission", Proceedings of 7<sup>th</sup> IFAC Robot Control 2003, vol. 1, pp. 85-90, Enslevier LTD, U.K., 2004.  
 Romano, V.F., and Trindade, E.C., 2004, "Modeling and Design of a Telerobotic Trolley for the TV Transmission", 4<sup>th</sup> Intern.. Symposium on Robotics and Automation - ISRA 2004, August 2004, Querétaro, Mexico, pp. 629-634.  
 Romano, V.F., and Trindade, E.C., 2005, "Dynamic Modeling of a High Speed Trolley for the TV Transmission", ABCM Symposium Series in Mechatronics, Vol. 2, pp. 242-249, Rio de Janeiro, 2006.  
 Sciavicco, L., Siciliano, B., "Modelling and Control of Robot Manipulators", 2 Edition, London, Springer, 2000.

## 8. RESPONSIBILITY NOTICE

The authors are the only responsible for the printed material included in this paper.